Influence of structural form on hydration-heat-induced temperature rise of precast concrete lining segments for a metro transit station

Yuzhen Han, Lei Zhang, and Jizhong He

- A metro transit station with multiring segmental lining was designed in Changchun, China. Because of the size of the precast concrete lining segment, heat from hydration of cement on the segments could not be neglected.
- This paper describes a heat of hydration analysis of a segment that was conducted using finite element analysis to examine the ability of the closed-cavity and solid forms to control temperature increases.
- The segment was numerically modeled using a summer ambient temperature of 25°C (77°F) and a winter ambient temperature of 10°C (50°F).

Concrete is a composite material composed of cement, water, aggregate, and admixtures.[1] During the concrete casting process, the exothermic chemical reaction between cement and water (hydration of cement) releases a large amount of heat.[2,3] The large amount of hydration heat generated in a short time leads to a rapid rise in the concrete temperature at its early age. The high temperatures (greater than 70°C [158°F]) can give rise to delayed ettringite formation, which could cause the concrete to expand and crack and, in turn, reduce its strength and durability.[4–6] Furthermore, in the interior of concrete, heat is trapped because of the poor thermal conductivity of concrete, whereas on the surface of concrete, heat is released into the atmosphere.[3,7] The trapped heat causes the temperature of the interior to be relatively higher than the surface temperature. The temperature gradient from the core to the surface leads to an internal restraint, which results in compressive stresses in the interior and tensile stresses in the surface.[8,9] Consequently, thermal cracks could occur as the restraint-induced tensile stress in concrete exceeds its tensile strength.

The American Concrete Institute (ACI)[10] defines mass concrete as "any volume of concrete with dimensions large enough to require that measures be taken to cope with generation of heat from hydration of the cement and attendant volume change to minimize cracking." In mass concrete structures, the nonuniform distribution of temperatures is particularly apparent. To control or avoid the risk of thermal cracking in mass concrete, its early-age temperatures must

be reduced.[7,11] In recent decades, engineers and scientists have made great efforts to reduce the internal temperature of concrete. Research has so far mainly focused on optimizing the raw materials in concrete (for example, developing low-heat cement[12–14]) and choosing casting methods (such as embedding cooling pipes[7,15–18]) to reduce the temperature in mass concrete. In contrast, scant attention has been paid to improving the structural form of mass concrete to avert excessively high temperatures. This paper describes research on the effect of structural form on hydration-heat-related changes in precast concrete lining segments for a metro transit station in Changchun, China, a location where conventional cast-in-place construction for mass concrete structures is interrupted by months of cold winter weather.

Reducing concrete temperature

There are two main types of methods of reducing the concrete temperature: precooling and postcooling methods.[19,20] Methods to precool concrete often involve the improvement of materials, the reduction of placing temperatures, or both material improvements and reduced placing temperatures. Material improvements involve adjusting the mixture proportions of ingredients in concrete or developing new materials to reduce or inhibit the release of hydration heat. For example, the content of cement may be reduced,[21–23] low-heat cement may be used,[12–14] or hydration heat inhibitor may be added.[24–26] Jia et al.[26] incorporated a microcapsule sustained-release-type hydration heat inhibitor into concrete and succeeded in decreasing its peak temperature by delaying the hydration of low-heat portland cement. The primary objective of reducing placing temperature is to decelerate the hydration of cement by cooling concrete-forming components (cement, water, and aggregate) before they are mixed to form concrete.[21,23,27–29] Aniskin et al.[30] used ice as a substitute for some of the water in concrete and found that this technique was useful for reducing the maximum concrete temperature.

Postcooling methods aim to lower the temperature of concrete while it is hydrating. Postcooling is mainly performed by circulating cold water in pipes embedded in concrete.[7,15–18] Tasri and Susilawati[7] concluded that cooling water temperature, space between cooling pipes, and coefficient of convections from cooling pipes to cooling water could be optimized to obtain a temperature distribution that resulted in thermal stresses being less than the tensile strength of concrete. In addition, other methods, such as layered casting[31–33] and strengthened curing,[34,35] have been adopted to reduce the temperature of concrete and avoid the risk of thermal cracking.

Metro transit station model

In China, urban rail transit has emerged as a growing form of transportation in recent decades as the nation has rapidly urbanized. For example, the total length of the rail transit network in Changchun, China, was 106.9 km (66.4 mi) in 2019 and is expected to expand to 235 km (146 mi) with 174 stations by 2024.[36] Notably, because Changchun is in the middle temperate zone, it has been necessary to take a four- to six-month winter break when conventional cast-in-place concrete techniques have been used for construction of metro transit stations. This winter break exerts considerable pressure on construction schedules. To shorten the construction time line for Metro Line 2 in Changchun, an innovative underground metro transit station design with fully precast concrete components was applied.[37,38] The station, which was constructed with a cut-and-cover method, is mainly composed of multiple rings of precast concrete lining segments (**Fig. 1**). The dimensions and mass of these segments are detailed in **Table 1**. Given the large dimensions, these

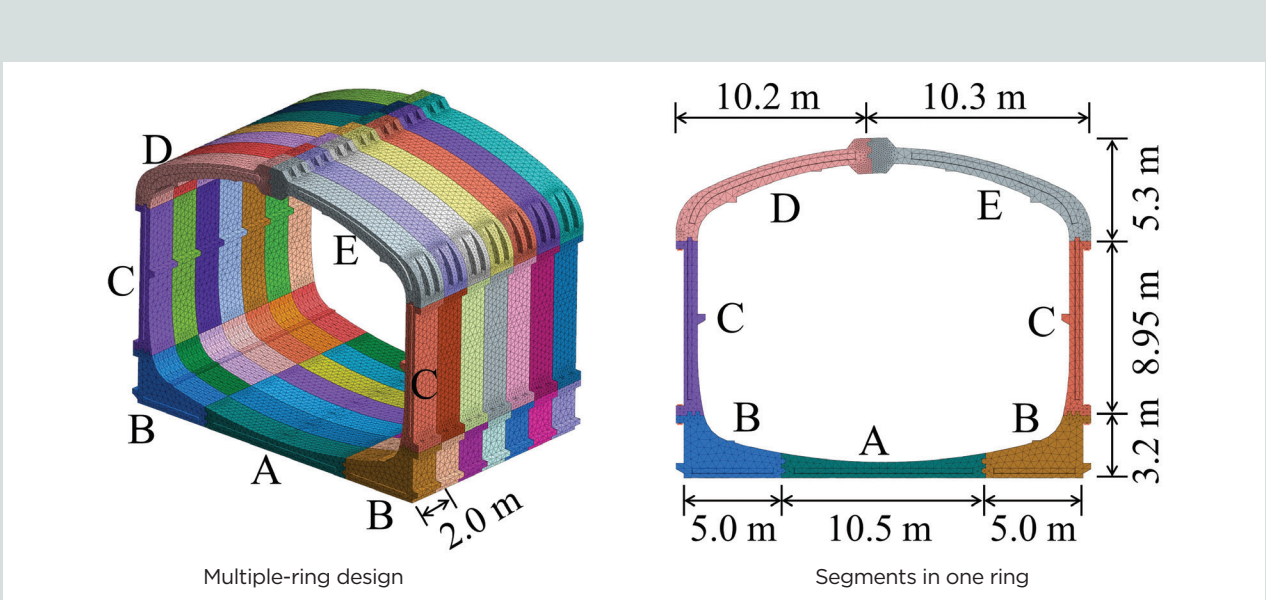

Figure 1. Lining segments for the precast concrete metro station. Note: 1 m = 3.281 ft.

Table 1. Information for the precast concrete lining segments

Segment	Length, m	Width, m	Thickness, m	Cavity volume, m³	Mass, tonne
A	10.50	0.80 to 1.26	2.00	4.60	40.0
B	5.00	3.20	2.00	6.00	40.0
C	8.95	0.70 to 1.02	2.00	1.74	31.0
D	10.20	5.30	2.00	4.71	48.5
E	10.30	5.30	2.00	4.77	54.5

Note: 1 m = 3.281 ft; 1 m³ = 1.308 yd³; 1 tonne = 1.102 tons.

segments were considered mass concrete structures; therefore, the effect of hydration heat during their casting could not be neglected.[39] To avert excessively high temperatures, the design included closed cavities in the interior of the segments. The closed cavities were located at the neutral zone, and the total volume proportion ranged from 15% to 22%. Reinforcement design was sufficient to ensure that each segment met strength requirements.[37]

The finite element method (FEM) can be an economical and powerful tool for accurately predicting the development of temperature and stress in mass concrete structures.[3,29,40,41] Using FEM, it is feasible to put forward effective measures for controlling the temperature in mass concrete structures at the design stage. In the study described in this paper, FEM was used to numerically simulate the development of temperature and stress in a precast concrete lining segment during its production. The FEM model and selected parameters were proved to be reasonable by comparing the temperature predictions with experimental temperature observations. To investigate the effect of the closed cavity on controlling the temperature rise, the segment was simulated in both closed-cavity and solid forms for comparison. The results from the finite element analysis were used to confirm whether the closed-cavity form could effectively control the temperature rise and the distributions of normal and shear stresses in the precast concrete segment.

Theoretical foundations of thermal analysis

This section introduces a differential equation of heat conduction, as well as initial and boundary conditions, to calculate the distribution of temperature in mass concrete.

Heat conduction equation

Heat conduction is the transfer of heat within a body due to temperature gradient. Given that concrete is isotropic and homogeneous, the heat conduction within it can be governed by the following equation:[42]

$$\frac{\partial T}{\partial t} - \frac{\lambda}{c\rho}\nabla^2 T = \frac{\partial \theta(t)}{\partial t}$$

where

T = temperature of the concrete

t = time

λ = thermal conductivity of concrete

c = specific heat of the concrete

ρ = density of the concrete

$\theta(t)$ = adiabatic temperature rise due to the heat from hydration of cement

The relation between $\theta(t)$ and t can be expressed by the following formula:[43]

$$\theta(t) = \theta_0(1 - e^{-mt})$$

where

θ_0 = the final value of the adiabatic temperature rise

m = rate coefficient of the adiabatic temperature rise

Initial condition

Initial temperature, which is the average temperature of water, cement, and aggregates at the time when concrete is placed, is the initial condition for thermal analysis. The initial temperature is continuously distributed in the concrete, and the concrete is assumed to be isothermal at the initial moment.[44]

Thermal boundary condition

To solve the differential equation governing heat conduction within a body, it is necessary to apply thermal conditions at the boundaries of the body. The three common boundary conditions are convection, specified temperature, and heat flux at the surface.[43] Convection is a form of heat transfer whereby heat is transmitted between a fluid (for example, water or air) and the surface of a solid through a fluid's relative molecular motion. In this study, convection was applied to consider the heat transmitted between the concrete surface and the atmosphere.[9,42,45] The heat transfer due to convection is governed by the following:

$$q_{conv} = h(T - T_a)$$

where

q_{conv} = convective heat flux

h = convection coefficient

T_a = ambient temperature

Finite element method model

The heat of hydration analysis in the study was carried out with a commercial FEM simulator (Midas/FEA). Segment B in Fig. 1 was selected for the hydration heat analysis and its three-dimensional FEMs in both solid and closed-cavity forms are presented in **Fig. 2**. The reinforcing bars were ignored in the models because their interaction with the concrete was beyond the scope of this work. The concrete mixture proportions of the lining segments were designed with a 28-day compressive strength of 50 MPa (7.25 ksi) (Grade C50) and the mixture components were determined according to the Chinese standard.[46] **Table 2** lists the main components of the concrete mixture. This study used common portland cement (**Table 3**).[47] **Table 4** presents the main model parameters for the heat of hydration analysis. The thermal properties of the concrete (thermal conductivity λ, specific heat c, convection coefficient h, final value of adiabatic temperature rise θ_0, rate coefficient of adiabatic temperature rise m, and coefficient of thermal expansion) were set to reasonable ranges from the

Table 2. Concrete mixture proportions

Component	Dosage, kg/m³
Cement	400
Fly ash	70
Ultra-fine sand	326
Medium-coarse sand	490
Gravel (5 to 10 mm)	379
Gravel (10 to 25 mm)	598
Water	150

Note: 1 mm = 0.0394 in.; 1 kg/m³ = 1.6875 lb/yd³.

Table 3. Portland cement mineral contents

	Ca_3SiO_5	Ca_2SiO_4	$Ca_3Al_2O_4$	$Ca_4Al_nFe_{2-n}O_7$
Proportion, %	40.62	29.58	10.42	9.15

Note: Al = aluminum; Ca = calcium; Fe = iron; O = oxygen; Si = silicon.

Table 4. Input parameters for the heat of hydration analysis

Parameter	Value
Thermal conductivity λ, kJ•m^{-1}•hr^{-1}•°C^{-1}	10.0
Specific heat c, kJ•kg^{-1}•°°C^{-1}	0.95
Density r, kg/m³	2400
Final value of adiabatic temperature rise θ_0, °C	56
Rate coefficient of adiabatic temperature rise m	0.45
Convection coefficient h, kJ•m^{-2}•hr^{-1}•°C^{-1}	50.4
Initial placing temperature T_0, °C	20
Ambient temperature in summer T_{as}, °C	25
Ambient temperature in winter T_{aw}, °C	10
Poisson's ratio	0.2
Coefficient of thermal expansion, °C^{-1}	1e^{-5}

Note: 1 kg/m³ = 1.6875 lb/yd³; 1 kJ/kg = 0.4299 Btu/lb; 1 kJ/m = 0.2889; 1 kJ/m² = 0.0881 Btu/ft²; °C = (°F – 32)1.8.

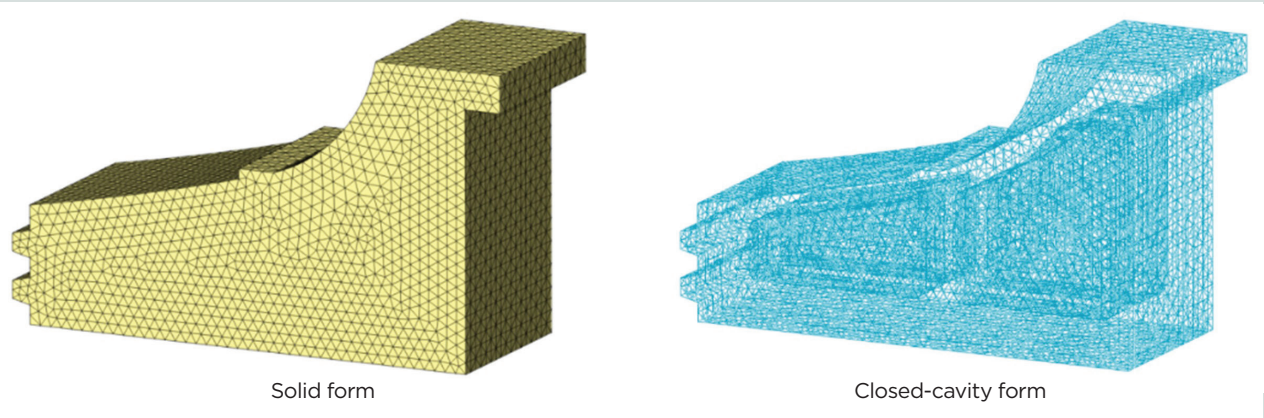

Figure 2. Finite element method models of segment B.

literature on similar materials.[48–52] Density ρ and Poisson's ratio were measured using the Chinese standard.[46] The initial temperature for placing concrete (the initial placing temperature T_0) was approximately maintained at 20°C (68°F). The ambient temperature T_a was specified or fixed during the manufacturing of the segments as either 25°C (77°F) for concrete being cast in the summer or 10°C (50°F) for winter casting.

Model validation

To validate the FEMs, the numerical predictions of temperature evolution in the closed-cavity segment B were compared with corresponding experimental observations. Two points around the surface and core of the closed-cavity segment B were selected to measure the evolution of temperature after concrete was placed. The corresponding measurement points in the numerical model and experimental observations were set at the same locations. **Figure 3** compares the evolution of temperature with time at the selected points in the numerical models and experimental measurements. The numerical predictions were approximately consistent with the experimental observations, although the temperature in the numerical model was slightly higher. This good consistency between the numerical and experimental results indicated that the FEM and selected parameters were reasonable.

Results

Figure 4 presents the temperature distributions in the closed-cavity and solid forms of segment B as the temperature rise reached its maximum (termed *maximum temperature distributions* herein) during 28 days of curing. Notably, for each specific structural form, the temperature of the segment cast in the summer was higher than the temperature of the segment cast in the winter. In each of the ambient temperatures, the temperature distribution in the closed-cavity segment was more uniform than that in the solid one. In both structural forms and at both ambient temperatures, the maximum temperatures of the segment occurred at the core.

To observe the evolution and differences of temperature in a segment, two points in each segment were designated to measure the evolution of temperature (Fig. 4). Points P1 and P2 were located at the core and surface of the segments, respectively, and were set at the same locations in each segment. **Figure 5** presents temperature history at the measurement points. Because of the heat from the hydration of the cement, the temperatures of all segments rapidly increased up to a peak, and then segment temperatures decreased to the value of the ambient temperature as hydration came to a halt. For the summer and winter ambient temperatures at both measurement points, the maximum temperature of the closed-cavity segment was much lower than that of the solid one and the peak temperature was reached earlier in the closed-cavity segment. These findings can be attributed to the lesser volume of concrete in the closed-cavity segment and hence the lesser amount of hydration heat.

When the summer ambient temperature was 25°C (77°F), the maximum temperatures at point P1 were 89.48°C (193.06°F) in the solid segment and 58.97°C (138.15°F) in the closed-cavity segment. Also at an ambient temperature of 25°C, the maximum temperatures at point P2 were 80.18°C (176.32°F) in the solid segment and 59.90°C (139.82°F) in the closed-cavity segment. In other words, compared with the maximum tem-

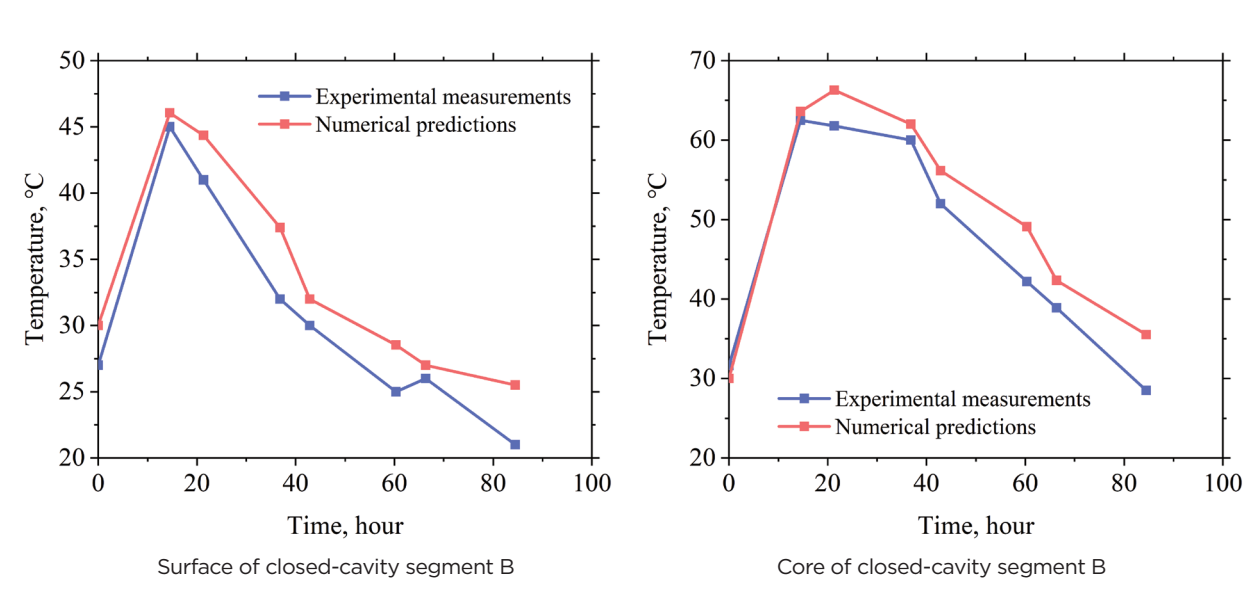

Figure 3. Comparison between the experimental measurements and numerical predictions of time-temperature history. Note: °C = (°F – 32)1.8.

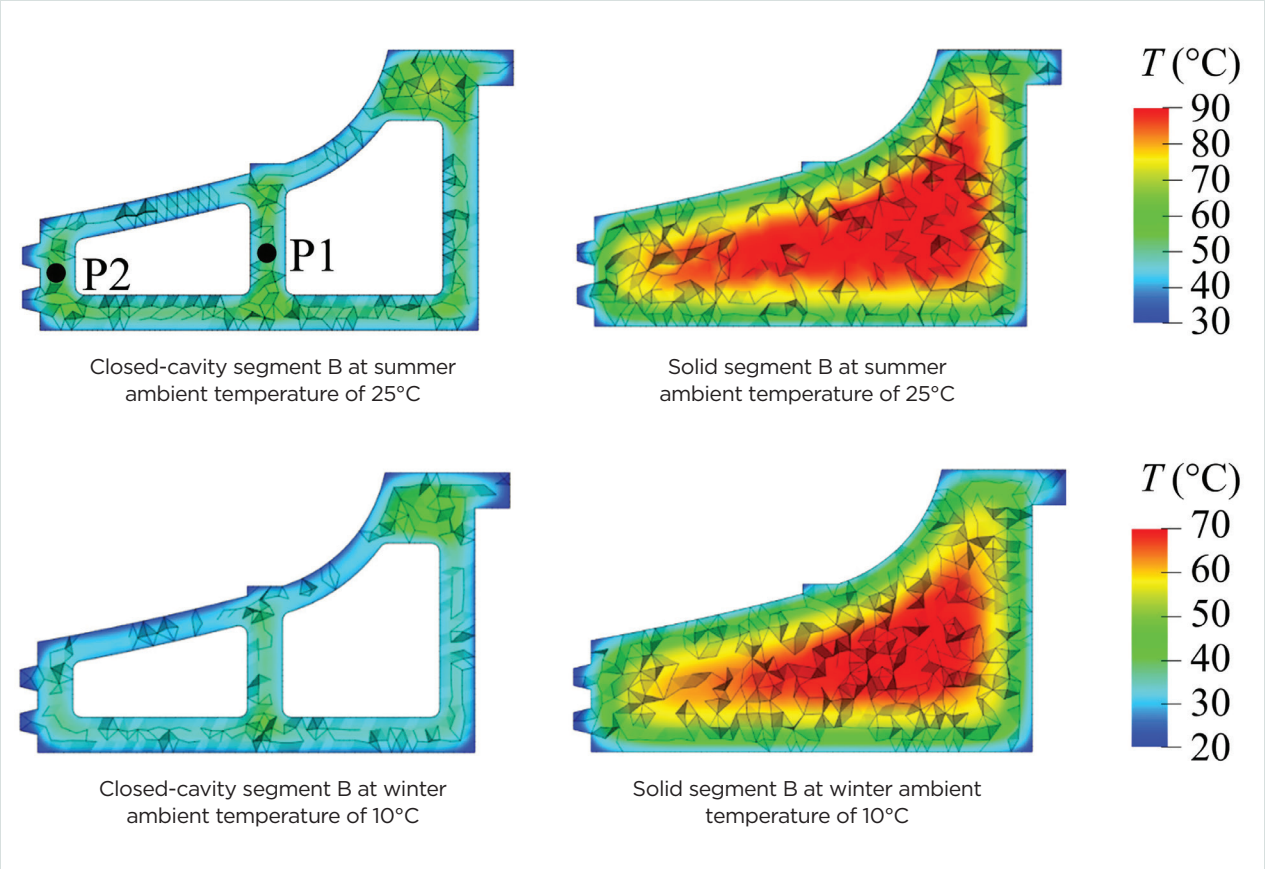

Figure 4. Maximum concrete temperature distributions of segment B forms. Note: P1 = temperature measurement point 1; P2 = temperature measurement point 2; *T* = temperature of concrete. °C = (°F – 32)1.8.

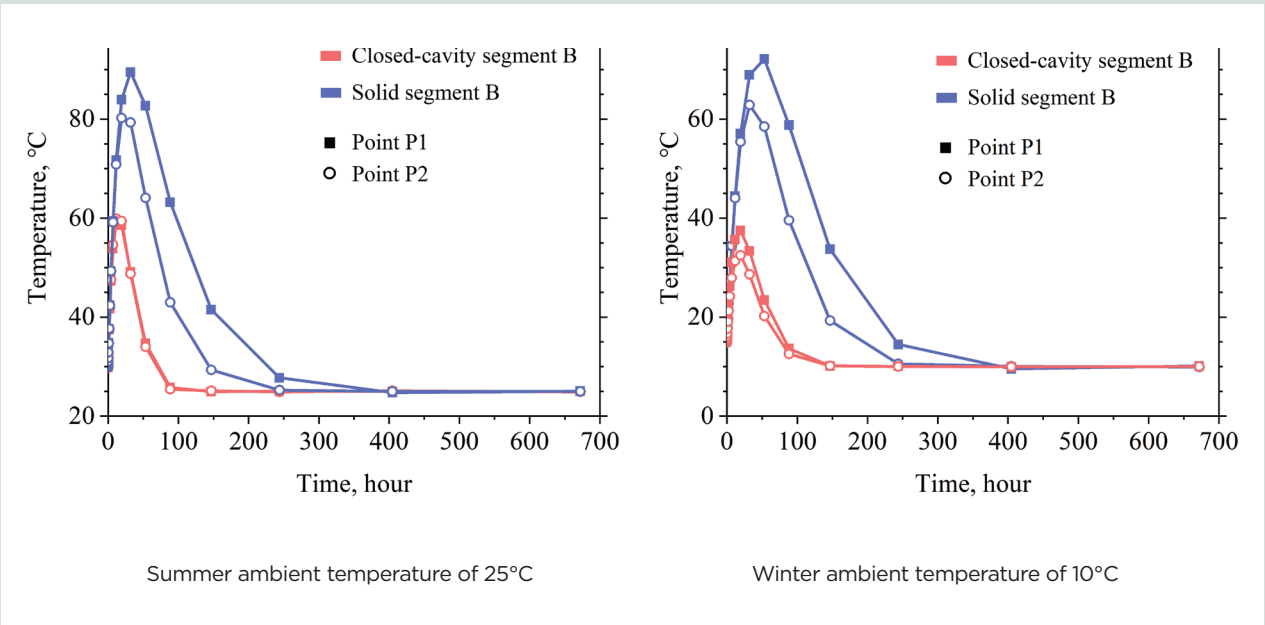

Figure 5. Time-temperature history at measurement points (P1, P2) of segment B forms. Note: °C = (°F – 32)1.8.

perature in the solid segment, the maximum temperature in the closed-cavity segment was approximately 31.4% lower at point P1 and 25.3% lower at point P2 in the summer scenario.

At the winter ambient temperature of 10°C (50°F) , the maximum temperatures at point P1 were 72.12°C (161.82°F) in the solid segment and 37.49°C (99.48°F) in the closed-cavity segment. The maximum temperatures at point P2 were 62.81°C (145.06°F) in the solid segment and 32.49°C (90.48°F) in the close-cavity segment. Thus, in the winter scenario, the maximum temperatures of the closed-cavity segment were approximately 48.0% lower at point P1 and 48.3% lower at point P2 than maximum temperatures at the same points in the solid segment.

Furthermore, at each of the ambient temperatures, the maximum temperature differences between point P1 and point P2 were smaller when the closed-cavity form was employed. In both the summer and winter scenarios, the maximum temperature difference between the two points was around 10°C (50°F) in the solid segment. In contrast, in the closed-cavity segment, the maximum temperature difference between P1 and P2 was about 5°C (41°F) when the ambient temperature was 10°C and almost negligible when the ambient temperature was 25°C (77°F). The lower temperatures and smaller temperature differences in the closed-cavity segment indicated that the closed-cavity form was more effective in suppressing the temperature rise, which lowered the risk of thermal cracking. ACI's *Guide to Mass Concrete*[10] says that to avoid the cracks caused by delayed ettringite formation and thermal stress, the maximum temperature and the temperature difference inside the concrete must not exceed 70°C and 20°C (158°F and 68°F), respectively. For this study, the temperatures during casting of the closed-cavity segment completely satisfied the ACI requirements and the maximum temperature of the solid segment exceeded the 70°C threshold for avoiding the risk of delayed ettringite formation.

Figures 6 and **7** present the distributions of normal and shear stresses in the segments as the stresses reach a maximum. (These stresses are termed *maximum normal stress distribution* and *maximum shear stress distribution* herein, respectively.)

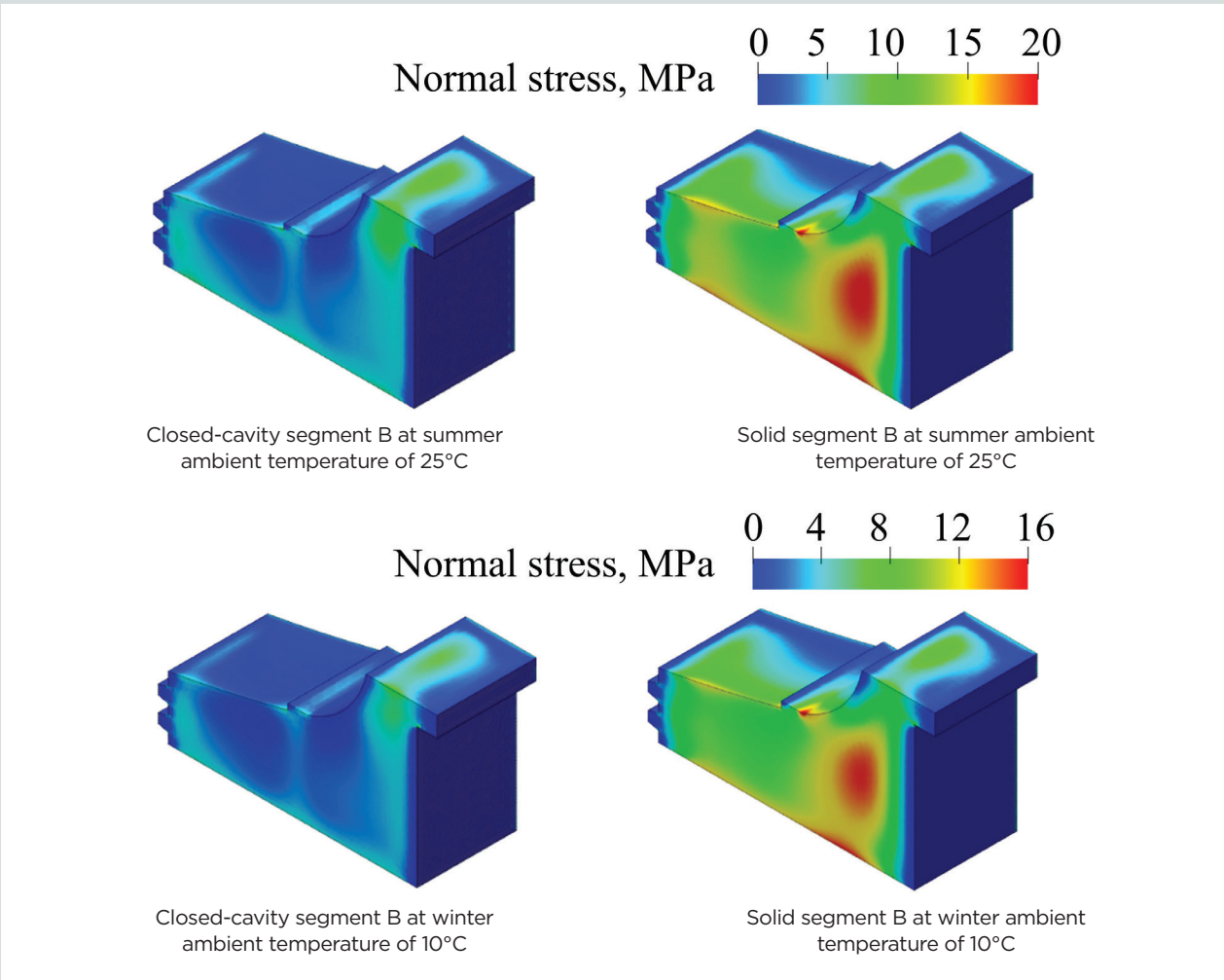

Figure 6. Maximum normal stress distributions of segment B forms. Note: 1 MPa = 0.145 ksi; °C = (°F – 32)1.8.

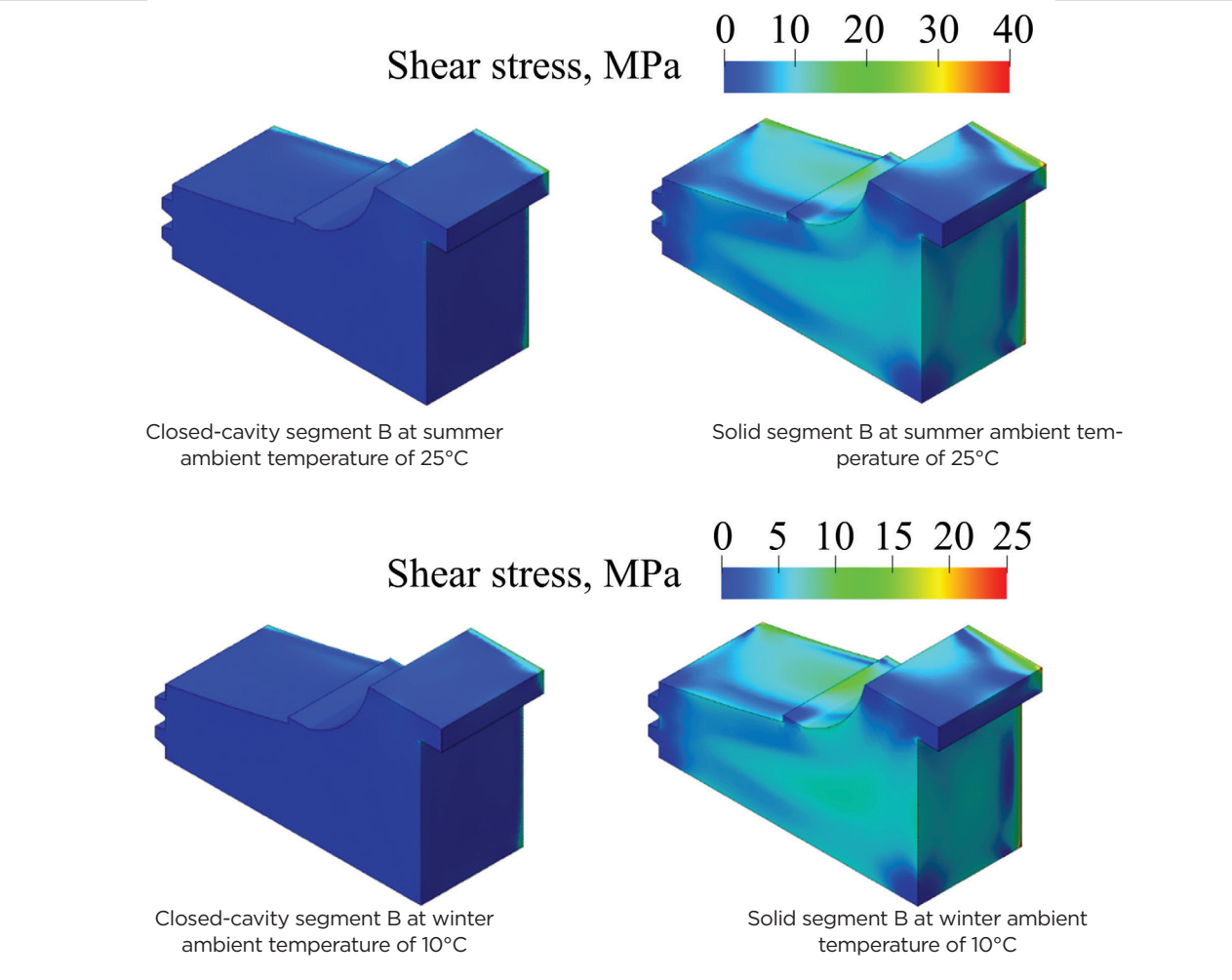

Figure 7. Maximum shear stress distributions of segment B forms. Note: 1 MPa = 0.145 ksi; °C = (°F – 32)1.8.

For each specific structural form, the normal (shear) stress of the segment cast in summer temperatures was larger than that in winter temperatures; also, at each ambient temperature, the stresses of the closed-cavity segment were smaller than those in the solid one.

At the summer ambient temperature of 25°C (77° F), the maximum normal stress was 40.4% lower in the closed-cavity segment than in the solid segment (10.2 MPa [1.5 ksi] compared with 17.1 MPa [2.5 ksi]). The maximum shear stress in the closed-cavity segment was 22.7 MPa (3.3 ksi), which was 30.2% lower than the maximum shear stress of 32.5 MPa (4.7 ksi) in the solid segment.

At the winter ambient temperature of 10°C (50°F), the maximum normal stress was 8.1 MPa (1.2 ksi) in the closed-cavity segment and 15.7 MPa (2.3 ksi) in the solid segment (that is, the maximum normal stress was 48.7% lower in the closed-cavity segment). The maximum shear stress was 15.7 MPa in the closed-cavity segment and 37.5% lower than the maximum shear stress of 25.1 MPa (3.6 ksi) in the solid segment.

The smaller stresses in the closed-cavity segment indicated greater effectiveness of the closed-cavity form to mitigate the thermal stress and ensure the quality of the manufactured segments.

Conclusion

An innovative, fully prefabricated metro transit station with a multiring segmental lining was designed to expedite construction in Changchun, China, where cold winter weather stops conventional cast-in-place construction for several months. The precast concrete lining segments with large dimensions were mass concrete structures, so the effect of heat from hydration of cement on the segments could not be neglected. To avert excessively high concrete temperatures due to hydration heat, which can lead to delayed ettringite formation– and thermal stress–related cracking, a closed-cavity form was designed for the segments. The segment was numerically modeled in both closed-cavity and solid forms for comparison. Ambient temperatures of 25°C and 10°C (77°F and 50°F) were selected to simulate summer and winter production conditions, respectively.

The FEM and selected parameters were proved reasonable by the consistency between the numerical predictions and experimental observations from the closed-cavity segment. The results show that for both the closed-cavity and solid structural forms, the temperature of the segment cast in summer conditions was higher than that in winter conditions. In both of the ambient temperatures, the maximum temperature was much lower in the closed-cavity segment than in the solid one and the temperature distribution in the closed-cavity segment was more uniform. The lower temperature and more uniform temperature distribution in the closed-cavity segment resulted in less thermal stress in the closed-cavity segment, thereby lowering the probability of thermal cracking.

During casting of the closed-cavity segment, the maximum temperature and the difference in maximum temperatures inside the concrete were kept below 70°C and 20°C (158°F and 68°F), respectively, fully satisfying the ACI requirements[10] for avoiding cracks caused by delayed ettringite formation and thermal stress. In contrast, the maximum temperature of the solid segment exceeded 70°C. Thus, compared with the solid segment, the closed-cavity segment can more effectively resist cracking. With the closed-cavity segments and novel prefabrication techniques, on which Yang and Lin[53] have elaborated, six fully prefabricated metro transit stations have been completed in Changchun, China. The prefabrication of these segments in cold ambient temperatures has been proved to be effective in accelerating the construction of metro transit stations in the cold regions. Moreover, this prefabricated construction could be a promising approach to improve time-efficiency of other large-scale underground construction projects, such as underground parking structures.

Acknowledgments

The work discussed in this paper is supported by the Science and Technology Project on Developing the Xiong'an New Area (grants 2021-07 and 2021-03).

References

1. Gagg, C. R. 2014. "Cement and Concrete as an Engineering Material: An Historic Appraisal and Case Study Analysis." Engineering Failure Analysis, no. 40, 114–140. https://doi.org/10.1016/j.engfailanal.2014.02.004.

2. Ng, P. L., J. S. Du, X. F. Luo, and F. T. K. Au. 2015. "Hydration Temperature Rise and Thermal Stresses Induced in Segment-on-Pier of Prestressed Concrete Box Girder Bridge." In *Proceedings of the Second International Conference on Performance-based and Life-cycle Structural Engineering*, 679–688. Brisbane, Australia: School of Civil Engineering, University of Queensland. https://doi.org/10.14264/uql.2016.1185.

3. Leon, G., and H.-L. Chen. 2021. "Thermal Analysis of Mass Concrete Containing Ground Granulated Blast Furnace Slag." *CivilEng* 2 (1): 254–271. https://doi.org/10.3390/civileng2010014.

4. Myuran, K., N. S. A. Wanigaratne, and M. T. R. Jayasinghe. 2015. "Strategies for Prevention of Delayed Ettringite Formation in Large Concrete Sections." *Engineer: Journal of the Institution of Engineers, Sri Lanka* 48 (2): 1–13. https://doi.org/10.4038/engineer.v48i2.6829.

5. Lubej, S., I. Anžel, P. Jelušič, L. Koseč, and A. Ivanič,. 2016. "The Effect of Delayed Ettringite Formation on Fine Grained Aerated Concrete Mechanical Properties." *Science and Engineering of Composite Materials* 23 (3): 325–334. https://doi.org/10.1515/secm-2012-0107.

6. Kawabata ,Y., N. Ueda, T. Miura, and S. Multon. 2021. "The Influence of Restraint on the Expansion of Concrete due to Delayed Ettringite Formation." *Cement and Concrete Composites*, no. 121, 104062. https://doi.org/10.1016/j.cemconcomp.2021.104062.

7. Tasri, A., and A. Susilawati. 2019. "Effect of Cooling Water Temperature and Space between Cooling Pipes of Post-Cooling System on Temperature and Thermal Stress in Mass Concrete." *Journal of Building Engineering*, no. 24, 100731. https://doi.org/10.1016/j.jobe.2019.100731.

8. Jeon, S.-J. 2008. "Advanced Assessment of Cracking due to Heat of Hydration and Internal Restraint." *Materials Journal* 105 (4): 325–333. https://doi.org/10.14359/19893.

9. Soo Geun, K. 2010. "Effect of Heat Generation from Cement Hydration on Mass Concrete Placement." Master of science thesis, Iowa State University, Ames. https://doi.org/10.31274/etd-180810-763.

10. ACI (American Concrete Institute) Committee 207. 2005. *Guide to Mass Concrete*. ACI 207.1R-05. Farmington Hills, MI: ACI.

11. Mizobuchi, T. 1998. "Discussion on the Experimental Evaluation of Reducing Effect of Thermal Stress of Expansive Additive Based on Uniaxial Restraint Testing Device." *JCI Conference* 20 (2):1051–1056.

12. Huang, Y., G. Liu G, S. Huang, R. Rao, and C. Hu. 2018. "Experimental and Finite Element Investigations on the Temperature Field of a Massive Bridge Pier Caused by the Hydration Heat of Concrete." *Construction and Building Materials*, no. 192, 240–252. https://doi.org/10.1016/j.conbuildmat.2018.10.128.

13. Xin, J., G. Zhang, Y. Liu, Z. Wang, N. Yang, Y. Wang, R. Mou, Y. Qiao, J. Wang, and Z. Wu. 2020. "Environmental Impact and Thermal Cracking Resistance of Low Heat Cement (LHC) and Moderate Heat Cement

(MHC) Concrete at Early Ages." *Journal of Building Engineering*, no. 32, 101668. https://doi.org/10.1016/j.jobe.2020.101668.

14. Lee, M. H., B. S. Khil, and H. D. Yun. 2014. "Influence of Cement Type on Heat of Hydration and Temperature Rise of the Mass Concrete." *Indian Journal of Engineering and Materials Sciences* 21 (5): 536–542.

15. Tasri, A., and A. Susilawati. 2019. "Effect of Material of Post-Cooling Pipes on Temperature and Thermal Stress in Mass Concrete. *Structures*, no. 20, 204–212. https://doi.org/10.1016/j.istruc.2019.03.015.

16. Kim, J. K., K. H. Kim, and J. K. Yang. 2001. "Thermal Analysis of Hydration Heat in Concrete Structures with Pipe-Cooling System." *Computers and Structures* 79 (2): 163–171. https://doi.org/10.1016/S0045-7949(00)00128-0.

17. Zuo, Z., Y. Hu, Q. Li, and L. Zhang. 2014. "Data Mining of the Thermal Performance of Cool-Pipes in Massive Concrete via In Situ Monitoring." *Mathematical Problems in Engineering* 2014 (5): 1–15. https://doi.org/10.1155/2014/985659 and errata https://doi.org/10.1155/2014/608179.

18. Liu, K., Z. Wang, C. Jin, F. Wang, and X. Lu. 2015. "An Experimental Study on Thermal Conductivity of Iron Ore Sand Cement Mortar." *Construction and Building Materials* 101 (1): 932–941. https://doi.org/10.1016/j.conbuildmat.2015.10.108.

19. ACI Committee 207. 2005. *Cooling and Insulating Systems for Mass Concrete*. ACI 207.4R-05 (Reapproved 2012). Farmington Hills, MI: ACI.

20. KCI (Korea Concrete Institute). 2009. *Standard Specification for Concrete*. [In Korean.] Seoul, South Korea: KCI.

21. Lee, M. H., B. S. Khil, and H. D. Yun. 2013. "Thermal Analysis of Hydration Heat in Mass Concrete with Different Cement Binder Proportions." *Applied Mechanics and Materials*, no. 372, 199–202. https://doi.org/10.4028/www.scientific.net/AMM.372.199.

22. Hu, J., Z. Ge, and K. Wang. 2014. "Influence of Cement Fineness and Water-to-Cement Ratio on Mortar Early-Age Heat of Hydration and Set Times." *Construction and Building Materials*, no. 50, 657–663. https://doi.org/10.1016/j.conbuildmat.2013.10.011.

23. Lagundžija, S., and M. Thiam. 2017. "Temperature Reduction during Concrete Hydration in Massive Structures." Master's thesis, KTH Royal Institute of Technology, Stockholm, Sweden.

24. Yang, K.-H., G.-D. Moon, and Y.-S. Jeon. 2016. "Implementing Ternary Supplementary Cementing Binder for Reduction of the Heat of Hydration of Concrete." *Journal of Cleaner Production*, no. 112, 845–852. https://doi.org/10.1016/j.jclepro.2015.06.022.

25. Makul, N., and G. Sua-iam. 2018. "Effect of Granular Urea on the Properties of Self-Consolidating Concrete Incorporating Untreated Rice Husk Ash: Flowability, Compressive Strength and Temperature Rise. *Construction and Building Materials*, no. 162, 489–502. https://doi.org/10.1016/j.conbuildmat.2017.12.023.

26. Jia, F., Y. Yao, and J. Wang. 2021. "Influence and Mechanism Research of Hydration Heat Inhibitor on Low-Heat Portland Cement." *Frontiers Materials*, no. 8, 697380. https://doi.org/10.3389/fmats.2021.697380.

27. Chen, Y.L., C. J. Wang, S. Y. Li, and L. J. Chen. 2003. "The Effect of Construction Designs on Temperature Field of a Roller Compacted Concrete Dam—A Simulation Analysis by a Finite Element Method." *Canadian Journal of Civil Engineering* 30 (6): 1153–1156. https://doi.org/10.1139/l03-076.

28. Zhou, H., Y. Zhou, C. Zhao, and Z. Liang. 2016. "Optimization of the Temperature Control Scheme for Roller Compacted Concrete Dams Based on Finite Element and Sensitivity Analysis Methods." *Civil Engineering Journal* 25 (3): 14. https://doi.org/10.14311/CEJ.2016.03.0014.

29. Sargam, Y., M. Faytarouni, K. Riding, K. Wang, C. Jahren, and J. Shen. 2019. "Predicting Thermal Performance of a Mass Concrete Foundation—A Field Monitoring Case Study." *Case Studies in Construction Materials*, no. 11, e00289. https://doi.org/10.1016/j.cscm.2019.e00289.

30. Aniskin, N., T. Chuc Nguyen, and A. Kiet Bui. 2021. "The Use of Ice to Cool the Concrete Mix in the Construction of Massive Structures." *E3S Web of Conferences*, no. 264, 02047. https://doi.org/10.1051/e3sconf/202126402047.

31. Chen, J., Z. Quan, and X. Peng. 2016. "Simulation Analysis on Mass Concrete Temperature Field of Lock Floor Layered Pouring." *Journal of Environmental Science and Engineering* 5 (9): 476–483. https://doi.org/10.17265/2162-5298/2016.09.006.

32. Han, S. 2020. "Assessment of Curing Schemes for Effectively Controlling Thermal Behavior of Mass Concrete Foundation at Early Ages." *Construction and Building Materials*, no. 230, 117004. https://doi.org/10.1016/j.conbuildmat.2019.117004.

33. Le, H.-H., C.-C. Vu, N.-K. Ho, and V.-T. Luu. 2020. "A Method of Controlling Thermal Crack for Mass Concrete

Structures: Modelling and Experimental Study." *IOP Conference Series: Materials Science and Engineering* 869 (7): 072054. https://doi.org/10.1088/1757-899X/869/7/072054.

34. Wang, X., Q. Chen, J. Tao, R. Han, X. Ding, F. Xing, and N. Han. 2019. "Concrete Thermal Stress Analysis during Tunnel Construction." *Advances in Mechanical Engineering* 11 (6): 168781401985223. https://doi.org/10.1177/1687814019852232

35. Jin, W., L. Jiang, L. Han, L. Chen, X. Yan, and C. Chen. 2021. "Influence of Curing Temperature on the Mechanical Properties and Microstructure of Limestone Powder Mass Concrete." *Structural Concrete* 22 (S1): E745–E755. https://doi.org/10.1002/suco.201900549

36. China's National Development and Reform Commission. Accessed January 17, 2023. "Reply to The Third Phase Construction Planning of Changchun Urban Rail Transit (2019–2024)." [In Chinese.] https://www.ndrc.gov.cn/fggz/zcssfz/zcgh/201812/t20181228_1145781.html.

37. Yang, X., and Y. Han. 2017. "Closed Cavity Thin-Wall Components Design for Prefabricated Underground Subway Structures." In *Geo-Risk 2017*, 194–205. Denver, CO: American Society of Civil Engineers. https://doi.org/10.1061/9780784480700.019.

38. Tao, L., P. Ding, C. Shi, X. Wu, S. Wu, and S. Li. 2019. "Shaking Table Test on Seismic Response Characteristics of Prefabricated Subway Station Structure." *Tunneling and Underground Space Technology*, no. 91, 102994. https://doi.org/10.1016/j.tust.2019.102994.

39. Central Research Institute of Building and Construction Co. 2018. *Standard for Construction of Mass Concrete*. [In Chinese.] Beijing, China: Ministry of Housing and Urban-Rural Construction of the People's Republic of China.

40. Lawrence, A.M., M. Tia, C. C. Ferraro, and M. Bergin. 2012. "Effect of Early Age Strength on Cracking in Mass Concrete Containing Different Supplementary Cementitious Materials: Experimental and Finite-Element Investigation." *Journal of Materials in Civil Engineering* 24 (4): 362–372. https://doi.org/10.1061/(ASCE)MT.1943-5533.0000389.

41. Yikici, T. A., and H.-L. Chen. 2015. "Numerical Prediction Model for Temperature Development in Mass Concrete Structures." *Transportation Research Record: Journal of the Transportation Research Board* 2508 (1): 102–110. https://doi.org/10.3141/2508-13.

42. Zhao, Y., G. Li, C. Fan, W. Pang, and Y. Wang. 2021. "Effect of Thermal Parameters on Hydration Heat Temperature and Thermal Stress of Mass Concrete." *Advances in Materials Science and Engineering*, vol. 2021, 1–16. https://doi.org/10.1155/2021/5541181.

43. Zhu, B. 2014. *Thermal Stresses and Temperature Control of Mass Concrete*. Boston, MA: Elsevier/Butterworth-Heinemann.

44. Zeng, H., C. Lu, L. Zhang, T. Yang, M. Jin, Y. Ma, and J. Liu. 2022. "Prediction of Temperature Distribution in Concrete under Variable Environmental Factors through a Three-Dimensional Heat Transfer Model." *Materials* 15 (4): 1510. https://doi.org/10.3390/ma15041510.

45. Lee, Y., M.-S. Choi, S.-T. Yi, and J.-K. Kim. 2009. "Experimental Study on the Convective Heat Transfer Coefficient of Early-Age Concrete." *Cement and Concrete Composites* 31 (1): 60–71. https://doi.org/10.1016/j.cemconcomp.2008.09.009.

46. China Academy of Building Research. 2011. *Specification for Mix Proportion Design of Ordinary Concrete*. [In Chinese.] Beijing, China: Ministry of Housing and Urban-Rural Construction of the People's Republic of China.

47. Xiong, Z., P. Wang, and Y. Wang. 2015. "Hydration Behaviors of Portland Cement with Different Lithologic Stone Powders." *International Journal of Concrete Structures and Materials* 9 (1): 55–60. https://doi.org/10.1007/s40069-014-0086-z.

48. Wang, H. L., and X. D. Zhang. 2015. "Study on the Effect of Fly Ash Mix Amount in Large Volume Pile Cap Concrete on Heat of Hydration." *Applied Mechanics and Materials*, vol. 744–746: 832–836. https://doi.org/10.4028/www.scientific.net/AMM.744-746.832.

49. Aniskin, N., C. Nguyen Trong, and L. Hoang Quoc. 2018. "Influence of Size and Construction Schedule of Massive Concrete Structures on Its Temperature Regime." *MATEC Web of Conferences*, no. 251, 02014. https://doi.org/10.1051/matecconf/201825102014.

50. Qiao, G., G. Xue, and G. Zhu. 2022. "A Precise Internal-Stress Calculation Algorithm for the Evolution of Cracking Risk of the Steam-Curing Box Girder." *Construction and Building Materials*, no. 346, 128463. https://doi.org/10.1016/j.conbuildmat.2022.128463.

51. Liu, L., S. Yu, W. Xu, and Z. Wang. 2021. "Study on Arrangement of Cooling Water Pipe to Control Hydration Heat of Concrete in Beam of Cable-Stayed Bridge." *Stavební Obzor—Civil Engineering Journal* 30 (2): 525–534. https://doi.org/10.14311/CEJ.2021.02.0039.

52. Xie, Y., C. Qian, Y. Xu, M. Wei, W. Du. 2022. "Effect of Fine Aggregate Type on Early-Age Performance, Cracking Analysis and Engineering Applications of C50 Concrete." *Construction and Building Materials*, no. 323, 126633. https://doi.org/10.1016/j.conbuildmat.2022.126633.

53. Yang, X., and F. Lin. 2021. "Prefabrication Technology for Underground Metro Station Structure." *Tunnelling and Underground Space Technology*, no. 108, 103717. https://doi.org/10.1016/j.tust.2020.103717.

Notation

c = specific heat of the concrete

h = convection coefficient

m = rate coefficient of adiabatic temperature rise

q_{conv} = convective heat flux

t = time

T = temperature of the concrete

T_a = ambient temperature

T_{as} = ambient temperature in summer

T_{aw} = ambient temperature in winter

T_0 = initial placing temperature

θ_0 = final value of adiabatic temperature rise

$\theta(t)$ = adiabatic temperature rise due to the heat from hydration of cement

λ = thermal conductivity of concrete

ρ = density of the concrete

About the authors

Yuzhen Han, PhD, is a structural engineering manager from Beijing Urban Construction Design and Development Group Co. Ltd. in Beijing, China.

Lei Zhang, PhD, is a geotechnical engineer from Beijing Urban Construction Group Co. Ltd.

Jizhong He is a geotechnical engineer from Beijing Urban Construction Design and Development Group Co. Ltd.

Abstract

This paper describes research on the effect of structural form on hydration-heat-related changes in large-scale precast concrete lining segments. These segments of mass concrete were used in the construction of an underground metro transit station in Changchun, China, a location where conventional cast-in-place construction is interrupted for months by cold winter weather. Heat of hydration analysis of closed-cavity and solid lining segments was conducted using the finite element method (FEM). Two ambient temperatures of 25°C and 10°C (77°F and 50°F) were selected to simulate segment manufacturing conditions in summer and winter, respectively. The FEM and selected parameters were found to be reasonable because the numerical predictions and experimental observations from the closed-cavity segment were consistent. At both of the ambient temperatures, the maximum internal concrete temperature of the closed-cavity segment was much lower than that in the solid one and the temperature distribution in the closed-cavity segment was more uniform. As a result, thermal stress was lower in the closed-cavity segment than in the solid segment, which reduced the risk for cracking. The closed-cavity form of the lining segments enhanced the structural integrity and durability, and the ability to prefabricate these segments in cold ambient temperatures effectively accelerated construction on this project.

Keywords

FEM, finite element method, heat of hydration, lining segment, prefabricated metro transit station, structural form, transit.

Review policy

This paper was reviewed in accordance with the Precast/Prestressed Concrete Institute's peer-review process. The Precast/Prestressed Concrete Institute is not responsible for statements made by authors of papers in *PCI Journal*. No payment is offered.

Publishing details

This paper appears in *PCI Journal* (ISSN 0887-9672) V. 68, No. 2, March–April 2023, and can be found at https://doi.org/10.15554/pcij68.2-04. *PCI Journal* is published bimonthly by the Precast/Prestressed Concrete Institute, 8770 W. Bryn Mawr Ave., Suite 1150, Chicago, IL 60631.

Reader comments

Please address any reader comments to *PCI Journal* editor-in-chief Tom Klemens at tklemens@pci.org or Precast/Prestressed Concrete Institute, c/o *PCI Journal*, 8770 W. Bryn Mawr Ave., Suite 1150, Chicago, IL 60631.